INVERSION OF THE BREMMER SERIES[*]

Hala A.H. Shehadeh

Department of Mathematics and Statistics, James Madison University, Harrisonburg, VA 22801
Email: alhajjhy@jmu.edu

Alison E. Malcolm

Earth Sciences Department, Memorial University of Newfoundland, St John's, Canada
Email: amalcolm@mun.ca

John C. Schotland

Department of Mathematics and Department of Physics, University of Michigan, Ann Arbor
MI 48109, USA
Email: schotland@umich.edu

Abstract

We consider the inverse backscattering problem for scalar waves in one dimension. We analyze the convergence of the inverse Bremmer series in this context and study its use in numerical simulations.

Mathematics subject classification: 78A46.
Key words: Inverse scattering.

1. Introduction

The inverse scattering problem (ISP) consists of recovering the spatially varying scattering potential of a bounded medium from measurements recorded on its boundary. In a typical experiment, a source creates a wave that is incident on the medium and the resulting scattered wave is collected by an array of detectors. There are many variants of this basic scenario. The source may be pulsed or time harmonic and the detector may be time or frequency resolved, polarization or phase sensitive, located in the near- or far-field and so on. There are numerous areas of application of the ISP ranging from seismic imaging of the earth to optical or ultrasonic imaging of the human body. We note that there is a considerable body of work on the ISP that has been been reviewed in [1–3]. Much is known about theoretical aspects of the problem, especially on matters of uniqueness, stability and partial data. There has also been significant effort devoted to the development of computational techniques to reconstruct the scattering potential. These include optimization methods, qualitative methods such as the linear sampling method, and direct approaches such as the $\bar{\partial}$-method and inversion of the Born series. The inverse Born series has been applied to inverse problems associated with the diffusion equation [4, 5], radiative transport equation [6] and the scalar wave equation [7]. In combination with a spectral method for solving the linear inverse problem, the inverse Born series leads to a fast image reconstruction algorithm with analyzable convergence, stability and error.

In this paper, we investigate the inverse of the Bremmer series for scalar waves. In contrast to the Born series, the Bremmer series allows for a directional decomposition of the wave field into up- and down-going components [8]. This decomposition is natural in the setting of

seismic imaging, where the Earth's subsurface is layered in the vertical direction. Inversion of the Bremmer series was proposed as a direct method for solving the ISP in [9]. Here we analyze the convergence, stability and approximation error of the method. We also illustrate its use in numerical simulations. We find that the series converges rapidly for low contrast objects. As the contrast is increased, the higher order terms systematically improve the reconstructions until, at sufficiently large contrast, the series diverges. We note that our analysis is restricted to one-dimension. The higher-dimensional case has a different mathematical structure and will be discussed elsewhere.

The remainder of this paper is organized as follows. In Section 2 we construct the Bremmer series for time-harmonic scalar waves in one dimension. We then derive various estimates that are used to study the convergence of the Bremmer series and its inverse. Inversion of the Bremmer series is discussed in Section 3. Numerical reconstructions are presented in Section 4. Finally, our conclusions are presented in Section 5.

2. Forward Problem

We begin by considering the one-dimensional wave equation on the real line for time-harmonic waves. The field u obeys

$$\partial_x^2 u + k_0^2(1 + \eta(x))u = 0, \tag{2.1}$$

where k_0 is the wave number and the scattering potential η is supported on the interval $[0, a]$. It will prove useful to decompose the field into the sum of an incident field and a scattered field:

$$u = u_0 + u_s. \tag{2.2}$$

The incident field will be taken to be a plane wave of the form

$$u_0(x) = e^{ik_0 x}. \tag{2.3}$$

The scattered field u_s satisfies

$$\partial_x^2 u_s + k_0^2 u_s = -k_0^2 \eta(x)u \tag{2.4}$$

and obeys the Sommerfeld radiation condition

$$\lim_{|x| \to \infty} (\partial_x u_s - ik_0 u_s) = 0. \tag{2.5}$$

The forward problem is to determine u for a given η and incident field.

In order to decompose the field u into its up- and down-going components, we express (2.1) in matrix form as

$$\begin{cases} (I\partial_x - A)\vec{U}' = 0, \\ (I\partial_x - A_0)\vec{U}_0' = 0, \end{cases} \tag{2.6}$$

where I is the 2×2 identity matrix,

$$A = \begin{pmatrix} 0 & 1 \\ -k_0^2(1 + \eta(x)) & 0 \end{pmatrix}, \quad A_0 = \begin{pmatrix} 0 & 1 \\ -k_0^2 & 0 \end{pmatrix}. \tag{2.7}$$

$$\vec{U}' = \begin{pmatrix} u \\ \partial_x u \end{pmatrix}, \quad \vec{U}_0' = \begin{pmatrix} u_0 \\ \partial_x u_0 \end{pmatrix}. \tag{2.8}$$

Subtracting the second equation in (2.6) from the first equation, we have

$$(I\partial_x - A_0)\delta\vec{U}' = \delta A\vec{U}', \tag{2.9}$$

where

$$\delta\vec{U}' = \vec{U}' - \vec{U}_0', \quad \delta A = A - A_0. \tag{2.10}$$

The directional decomposition of u is now obtained by diagonalizing the matrix A_0:

$$A_0 = PD_0P^{-1} := \frac{1}{2}\begin{pmatrix} 1 & 1 \\ ik_0 & -ik_0 \end{pmatrix}\begin{pmatrix} ik_0 & 0 \\ 0 & -ik_0 \end{pmatrix}\begin{pmatrix} 1 & -i/k_0 \\ 1 & i/k_0 \end{pmatrix}. \tag{2.11}$$

Hence, (2.9) becomes

$$(I\partial_x - D_0)\delta\vec{U} = P^{-1}\delta AP\vec{U}, \tag{2.12}$$

where

$$\delta\vec{U} := \begin{pmatrix} \delta u_+ \\ \delta u_- \end{pmatrix} = P^{-1}\delta\vec{U}', \tag{2.13}$$

$$\vec{U} := \begin{pmatrix} u_+ \\ u_- \end{pmatrix} = P^{-1}\vec{U}'. \tag{2.14}$$

We thus have

$$\delta\vec{U} := \begin{pmatrix} \delta u_+ \\ \delta u_- \end{pmatrix} = P^{-1}\begin{pmatrix} u - u_0 \\ u_x - u_{0_x} \end{pmatrix} = \frac{1}{2}\begin{pmatrix} u - u_0 - \frac{i}{k_0}u_x + \frac{i}{k_0}u_{0_x} \\ u - u_0 + \frac{i}{k_0}u_x - \frac{i}{k_0}u_{0_x} \end{pmatrix}, \tag{2.15}$$

$$\vec{U} := \begin{pmatrix} u_+ \\ u_- \end{pmatrix} = P^{-1}\begin{pmatrix} u \\ u_x \end{pmatrix} = \frac{1}{2}\begin{pmatrix} u - \frac{i}{k_0}u_x \\ u + \frac{i}{k_0}u_x \end{pmatrix}. \tag{2.16}$$

Rewriting each component of (2.12) using the above notation, we obtain two coupled first order equations for δu_+ and δu_- of the form

$$\begin{cases} (\partial_x - ik_0)\delta u_+ = \dfrac{ik_0}{2}\eta(x)(u_+ + u_-), \\ (\partial_x + ik_0)\delta u_- = -\dfrac{ik_0}{2}\eta(x)(u_+ + u_-). \end{cases} \tag{2.17}$$

Using the fact that from (2.16), $u_+ + u_- = u$, (2.17) becomes

$$\begin{cases} (\partial_x - ik_0)\delta u_+ = \dfrac{ik_0}{2}\eta(x)u, \\ (\partial_x + ik_0)\delta u_- = -\dfrac{ik_0}{2}\eta(x)u. \end{cases} \tag{2.18}$$

We note that Eqs. (2.18) are coupled through (2.15) by the relation

$$\delta u_+ + \delta u_- = u - u_0. \tag{2.19}$$

We also note that the solution of (2.1) is $u = u_0 + \delta u_+ + \delta u_-$. Hence, u is the sum of the incident wave u_0, and the scattered field $\delta u_+ + \delta u_-$, where the scattered field is split into up- and down-going waves.

2.1. Green's functions

In order to solve Eqs. (2.18), we need to compute the Green's functions $G_+(x, y)$ and $G_-(x, y)$ corresponding to the inverses of the operators $\partial_x - ik_0$ and $\partial_x + ik_0$, respectively. The Green's functions satisfy

$$\partial_x G_+(x, y) + ik_0 G_+(x, y) = -\delta(x - y), \tag{2.20}$$

$$\partial_x G_-(x, y) - ik_0 G_-(x, y) = \delta(x - y) \tag{2.21}$$

and are taken to obey the radiation condition. It is easily seen that G_+ is given

$$G_+(x, y) = \begin{cases} 0 & \text{if } x > y, \\ -e^{ik_0(y-x)} & \text{if } x < y. \end{cases} \tag{2.22}$$

We also find that G_- is given by

$$G_-(x, y) = \begin{cases} e^{ik_0(x-y)} & \text{if } x > y, \\ 0 & \text{if } x < y. \end{cases} \tag{2.23}$$

Using the above results, we see that the solutions of Eqs. (2.18) are of the form

$$\begin{cases} \delta u_+(x) = \dfrac{ik_0}{2} \displaystyle\int_{-\infty}^{\infty} G_+(x, y)\eta(y)(u_0(y) + \delta u_+(y) + \delta u_-(y))dy, \\ \delta u_-(x) = \dfrac{ik_0}{2} \displaystyle\int_{-\infty}^{\infty} G_-(x, y)\eta(y)(u_0(y) + \delta u_+(y) + \delta u_-(y))dy. \end{cases} \tag{2.24}$$

2.2. Forward series

We are now ready to construct the series solution of the forward problem. The series we obtain is for the vector $\delta\vec{U}$, although we will be only interested in the second component δu_-, which corresponds to the reflected wave. We begin by expressing (2.24) in matrix notation as

$$\delta\vec{U}(x) = \frac{ik_0}{2} \int_{-\infty}^{\infty} \binom{G_+}{G_-}(x, y)u_0(y)\eta(y)dy + \frac{ik_0}{2} \int_{-\infty}^{\infty} \begin{pmatrix} G_+ & G_+ \\ G_- & G_- \end{pmatrix}(x, y) \binom{\delta u_+}{\delta u_-}(y)\eta(y)dy, \tag{2.25}$$

which can be rewritten as

$$\delta\vec{U}(x) = \frac{1}{2}\frac{ik_0}{2} \int_{-\infty}^{\infty} B(x, y)\mathbf{1}u_0(y)\eta(y)dy + \frac{ik_0}{2} \int_{-\infty}^{\infty} B(x, y)\delta\vec{U}(y)\eta(y)dy, \tag{2.26}$$

where $\mathbf{1} = (1, 1)^T$ and

$$B(x, y) = \begin{pmatrix} G_+(x, y) & G_+(x, y) \\ G_-(x, y) & G_-(x, y) \end{pmatrix}. \tag{2.27}$$

We now apply fixed point iteration to (2.26) to obtain a series solution of the integral equation (2.26).

$$
\begin{aligned}
\delta\vec{U}(x) = {} & \frac{1}{2}\frac{ik_0}{2}\int_{-\infty}^{\infty} B(x,y)\eta(y)\mathbf{1}u_0(y)dy \\
& + \frac{1}{2}\left(\frac{ik_0}{2}\right)^2 \int_{-\infty}^{\infty}\int_{-\infty}^{\infty} B(x,y_1)\eta(y_1)B(y_1,y)\eta(y)\mathbf{1}u_0(y)dydy_1 \\
& + \frac{1}{2}\left(\frac{ik_0}{2}\right)^3 \int_{-\infty}^{\infty}\int_{-\infty}^{\infty}\int_{-\infty}^{\infty} B(x,y_2)\eta(y_2)B(y_2,y_1)\eta(y_1)B(y_1,y)\eta(y) \\
& \qquad \times \mathbf{1}u_0(y)dydy_1dy_2 \\
& + \cdots .
\end{aligned}
\tag{2.28}
$$

Note that $\eta(x)$ is supported on the interval $[0,a]$. The ranges of integration in (2.28) can accordingly be restricted $[0,a]$.

It will prove convenient to express the series (2.28) as a formal series in tensor powers of η of the form

$$
\delta\vec{U} = K_1\eta + K_2\eta\otimes\eta + K_3\eta\otimes\eta\otimes\eta + \cdots .
\tag{2.29}
$$

The operators K_n are defined by

$$
\begin{aligned}
(K_nf)(k_0) = {} & \frac{1}{2}\left(\frac{ik_0}{2}\right)^n \int_0^a \cdots \int_0^a B(x,y_{n-1})B(y_{n-1},y_{n-2})\ldots B(y_1,y) \\
& \times f(y,y_1,\ldots,y_{n-1})\mathbf{1}u_0(y)dydy_1\cdots dy_{n-1},
\end{aligned}
\tag{2.30}
$$

where the point $x \in \mathbb{R}$ at which the field is measured is fixed. Here the dependence of the forward operators K_n on the wavenumber k_0 has been made explicit and the dependence on the coordinate x has been suppressed. This will come in handy when we study the inverse problem with frequency-dependent data. We note that δu_-, which is the second component of $\delta\vec{U}$, is given by the series

$$
\delta u_- = K_{12}\eta + K_{22}\eta\otimes\eta + K_{32}\eta\otimes\eta\otimes\eta + \cdots .
\tag{2.31}
$$

Here K_{nm} denotes component m of the operator K_n. We will refer to (2.29) as the Bremmer series. It is written in a somewhat different form than in the original paper by Bremmer [8], but is closely related to the generalized Bremmer series in [9].

2.3. Convergence of the Bremmer series

We now consider the convergence of the Bremmer series. We will require the following elementary estimate on the norm of the operator K_n.

Lemma 2.1. *Let* $X = [0,a]$ *and* $Y = [0,k_{max}]$. *The operator*

$$
K_{nm} : L^\infty(X \times \cdots \times X) \longrightarrow L^\infty(Y), \quad m = 1,2
$$

defined by (2.30) *is bounded and*

$$
\|K_{nm}\| \le \nu\mu^{n-1},
$$

where

$$
\mu = k_{max}a, \quad \nu = \frac{1}{2}k_{max}a.
\tag{2.32}
$$

Using the above lemma, we obtain the following result on the convergence of the Bremmer series.

Proposition 2.1. *If the smallness condition $\|\eta\|_{L^\infty(X)} < 1/\mu$ holds, then the components of the Bremmer series* (2.29) *converge in L^∞.*

Proof. To show that the Bremmer series converges, we estimate the sum

$$\sum_n \|K_{nm}\eta \otimes \cdots \otimes \eta\|_{L^\infty(Y)} \tag{2.33}$$

by a geometric series. We thus have

$$\sum_n \|K_{nm}\eta \otimes \cdots \otimes \eta\|_{L^\infty(Y)}$$
$$\leq \sum_n \|K_{nm}\|\|\eta\|_{L^\infty(X)}^n \leq \frac{\nu}{\mu}\sum_n \left(\mu\|\eta\|_{L^\infty(X)}\right)^n, \tag{2.34}$$

which converges if $\mu\|\eta\|_{L^\infty(X)} < 1$. $\square$

3. Inverse Problem

The inverse problem is to determine the scattering potential $\eta(x)$ for $x > 0$ from measurements of δu_- at $x = 0$ for wavenumbers $k_0 \in [0, k_{\max}]$. Physically, such measurements correspond to recording the amplitude and phase of the reflected wave at the origin. Following [4], we express η as a series in tensor powers of δu_- of the form

$$\eta = \mathcal{K}_1\delta u_- + \mathcal{K}_2\delta u_- \otimes \delta u_- + \mathcal{K}_3\delta u_- \otimes \delta u_- \otimes \delta u_- + \cdots, \tag{3.1}$$

where the inverse operators $\mathcal{K}_j : L^\infty(Y \times \cdots \times Y) \longrightarrow L^\infty(X)$ are given by

$$\mathcal{K}_1 K_{12} = I, \tag{3.2a}$$

$$\mathcal{K}_2 = -\left(\mathcal{K}_1 K_{22}\right)\mathcal{K}_1 \otimes \mathcal{K}_1, \tag{3.2b}$$

$$\mathcal{K}_3 = -\left(\mathcal{K}_2 K_{12} \otimes K_{22} + \mathcal{K}_2 K_{22} \otimes K_{12} + \mathcal{K}_1 K_{32}\right)\mathcal{K}_1 \otimes \mathcal{K}_1 \otimes \mathcal{K}_1. \tag{3.2c}$$

For $n > 3$ we have

$$\mathcal{K}_n = -\left(\sum_{m=1}^{n-1} \mathcal{K}_m \sum_{i_1 + \cdots + i_m = n} K_{i_12} \otimes \cdots \otimes K_{i_m2}\right)\mathcal{K}_1 \otimes \cdots \otimes \mathcal{K}_1. \tag{3.3}$$

We will refer to (3.1) as the inverse Bremmer series.

The operator $\mathcal{K}_1$ is the regularized pseudoinverse of K_{12}. It is defined as follows. Consider the Tikhonov functional T which is given by

$$T(\eta) = \|K_{12}\eta - \delta u_-\| + \alpha F(\eta), \tag{3.4}$$

where F is a convex penalty function and $\alpha > 0$ is a regularization parameter [10, 11]. The minimizer of T is denoted $\eta^\dagger$ and is referred to as the regularized pseudoinverse solution of $K_{12}\eta = \delta u_-$. The operator $\mathcal{K}_1$ is defined as the map $\mathcal{K}_1 : \phi \mapsto \eta^\dagger$. Here we take $\eta \in X$, where

X is a smooth and uniformly convex subspace of $L^\infty(X)$. Since K_1 is bounded, it follows that $\eta^\dagger$ exists and is unique.

The inverse Born series was analyzed in [4]. It was shown that if the forward operators obey certain norm estimates, then the inverse Born series converges and its error and stability can be analyzed. The same analysis applies to the inverse Bremmer series. We characterize the convergence of the inverse Bremmer series as follows. Let $H := \max(\|\eta\|_{L^\infty(X)}, \|\mathcal{K}_1 K_1 \eta\|_{L^\infty(X)})$ and assume that $\|\mathcal{K}_1\|_\infty < 1/(\mu + \nu)$, $\|\mathcal{K}_1 \delta u_-\|_{L^\infty(X)} < 1/(\mu + \nu)$ and $H < 1/(\nu + \mu)$. Then the inverse Bremmer series converges and the following error estimate holds:

$$\left\| \eta - \sum_{n=1}^N \mathcal{K}_n \delta u_- \otimes \cdots \otimes \delta u_- \right\|_{L^\infty(X)}$$

$$\leq C \|(I - \mathcal{K}_1 K_1)\eta\|_{L^\infty(X)} + \tilde{C} \frac{[(\mu+\nu)\|\mathcal{K}_1 \delta u_-\|_{L^\infty(X)}]^{N+1}}{1 - (\mu+\nu)\|\mathcal{K}_1 \delta u_-\|_{L^\infty(X)}}, \tag{3.5}$$

where $C = C(\mu, \nu, \|\mathcal{K}_1\|_\infty, H)$ and $\tilde{C} = \tilde{C}(\mu, \nu, \|\mathcal{K}_1\|_\infty)$ are independent of N and δu_-.

Remark 3.1. We emphasize that $\mathcal{K}_1$ is the regularized pseudoinverse of K_{12}. As a consequence, the inverse Bremmer series does not converge to the coefficient η. However, if η is known a priori to belong to the subspace on which it is possible to invert K_{12}, then the limit of the series coincides precisely with η. Further discussion of this point is provided in [4].

4. Numerical Results

In this section we present the numerical reconstructions of two model systems. The first system has scattering potential η of the form

$$\eta(x) = \begin{cases} \dfrac{c_0^2}{c_1^2} - 1 & \text{if} \quad 0 \leq x \leq a, \\ 0 & \text{otherwise.} \end{cases} \tag{4.1}$$

The field then obeys the wave equations, interface and boundary conditions

$$\partial_x^2 u_1 + k_0^2 u_1 = 0 \qquad \text{in} \quad (-\infty, 0), \tag{4.2a}$$

$$\partial_x^2 u_2 + k_1^2 u_2 = 0 \qquad \text{in} \quad [0, a], \tag{4.2b}$$

$$\partial_x^2 u_3 + k_0^2 u_3 = 0 \qquad \text{in} \quad (a, \infty), \tag{4.2c}$$

$$u_1(0) = u_2(0), \qquad \partial_x u_1(0) = \partial_x u_2(0), \tag{4.2d}$$

$$u_2(a) = u_3(a), \qquad \partial_x u_2(a) = \partial_x u_3(a), \tag{4.2e}$$

$$\lim_{x \to \infty} (\partial_x u_3 - ik_0 u_3) = 0. \tag{4.2f}$$

where $k_0 = \omega/c_0$ and $k_1 = \omega/c_1$. It is easily seen that the solutions to the above equations are of the form

$$u_1(x) = e^{ik_0 x} + R_1 e^{-ik_0 x}, \tag{4.3a}$$

$$u_2(x) = R_2 e^{-ik_1 x} + T_2 e^{ik_1 x}, \tag{4.3b}$$

$$u_3(x) = T_3 e^{ik_0 x}. \tag{4.3c}$$

Here the reflection and transmission coefficients are given by

$$R_1 = \frac{(k_0^2 - k_1^2)\sin(k_1 a)}{2ik_0 k_1 \cos(k_1 a) + (k_0^2 + k_1^2)\sin(k_1 a)}, \tag{4.4a}$$

$$R_2 = \frac{2k_0(k_0 - k_1)e^{2ik_1 a}}{e^{2ik_1 a}(k_0 - k_1)^2 - (k_0 + k_1)^2}, \tag{4.4b}$$

$$T_2 = -\frac{2k_0(k_0 + k_1)}{e^{2ik_1 a}(k_0 - k_1)^2 - (k_0 + k_1)^2}, \tag{4.4c}$$

$$T_3 = \frac{2ik_0 k_1 e^{-ik_0 a}}{2ik_0 k_1 \cos(k_1 a) + (k_0^2 + k_1^2)\sin(k_1 a)}. \tag{4.4d}$$

The scattering data consists of measurements of δu_- at $x = 0$ for wave numbers $k_0 \in [0, k_{\max}]$, where $k_{\max} a = 3$. It follows immediately from (4.8a) that

$$\delta u_-(0) = R_1. \tag{4.5}$$

The second system has a scattering potential of the form

$$\eta(x) = \begin{cases} \dfrac{c_0^2}{c_1^2} - 1 & \text{if} \quad 0 \le x \le a, \\[2ex] \dfrac{c_0^2}{c_2^2} - 1 & \text{if} \quad a < x \le b, \\[2ex] 0 & \text{otherwise.} \end{cases} \tag{4.6}$$

The field then obeys the wave equations, interface and boundary conditions

$$\partial_x^2 u_1 + k_0^2 u_1 = 0 \qquad \text{in} \quad (-\infty, 0), \tag{4.7a}$$

$$\partial_x^2 u_2 + k_1^2 u_2 = 0 \qquad \text{in} \quad [0, a], \tag{4.7b}$$

$$\partial_x^2 u_3 + k_2^2 u_3 = 0 \qquad \text{in} \quad [a, b], \tag{4.7c}$$

$$\partial_x^2 u_4 + k_0^2 u_4 = 0 \qquad \text{in} \quad (b, \infty), \tag{4.7d}$$

$$u_1(0) = u_2(0), \qquad \partial_x u_1(0) = \partial_x u_2(0), \tag{4.7e}$$

$$u_2(a) = u_3(a), \qquad \partial_x u_2(a) = \partial_x u_3(a), \tag{4.7f}$$

$$u_3(b) = u_4(b), \qquad \partial_x u_3(b) = \partial_x u_4(b), \tag{4.7g}$$

$$\lim_{x \to \infty} (\partial_x u_4 - ik_0 u_4) = 0. \tag{4.7h}$$

where $k_0 = \omega/c_0$, $k_1 = \omega/c_1$ and $k_2 = \omega/c_2$. It is easily seen that the solutions to the above equations are of the form

$$u_1(x) = e^{ik_0 x} + R_1 e^{-ik_0 x}, \tag{4.8a}$$

$$u_2(x) = R_2 e^{-ik_1 x} + T_2 e^{ik_1 x}, \tag{4.8b}$$

$$u_3(x) = R_3 e^{-ik_2 x} + T_3 e^{ik_2 x}, \tag{4.8c}$$

$$u_4(x) = T_4 e^{ik_0 x}. \tag{4.8d}$$

Here the reflection and transmission coefficients are given by

$$R_1 = N_1/D_1, \quad R_2 = N_2/D_1, \tag{4.9a}$$

$$R_3 = N_3/D_2, \quad T_2 = N_4/D_1, \tag{4.9b}$$

$$T_3 = N_5/D_2, \quad T_4 = N_6/D_2, \tag{4.9c}$$

where $N_1, N_2, N_3, N_4, N_5, N_6, D_1$ and D_2 are defined by

$$N_1 = k_2 \left(k_1{}^2 - k_0{}^2\right) \sin(ak_1) \cos(k_2(a - b)) + \sin(k_2(a - b))\Big(k_1(k_0 - k_2)(k_0 + k_2)$$
$$\cos(ak_1) + ik_0(k_1 - k_2)(k_1 + k_2) \sin(ak_1)\Big), \tag{4.10a}$$

$$N_2 = k_0 e^{iak_1} \Big(\left(k_0 k_1 - k_2{}^2\right) \sin(k_2(a - b)) + ik_2(k_0 - k_1) \cos(k_2(a - b))\Big), \tag{4.10b}$$

$$N_3 = k_0 k_1 e^{ibk_2} (k_2 - k_0), \tag{4.10c}$$

$$N_4 = e^{-iak_1} \Big(k_0 \left(k_0 k_1 + k_2{}^2\right) \sin(k_2(a - b)) - ik_0 k_2(k_0 + k_1) \cos(k_2(a - b))\Big), \tag{4.10d}$$

$$N_5 = k_0 k_1 e^{-ibk_2} (k_0 + k_2), \quad N_6 = -2ik_0 k_1 k_2 e^{-ibk_0}, \tag{4.10e}$$

$$D_1 = \sin(k_2(a - b))\Big(k_1 \left(k_0{}^2 + k_2{}^2\right) \cos(ak_1) - ik_0 \left(k_1{}^2 + k_2{}^2\right) \sin(ak_1)\Big)$$
$$- k_2 \cos(k_2(a - b))\Big(\left(k_0{}^2 + k_1{}^2\right) \sin(ak_1) + 2ik_0 k_1 \cos(ak_1)\Big), \tag{4.10f}$$

$$D_2 = \sin(k_2(a - b))\Big(k_0 \left(k_1{}^2 + k_2{}^2\right) \sin(ak_1) + ik_1 \left(k_0{}^2 + k_2{}^2\right) \cos(ak_1)\Big)$$
$$- ik_2 \cos(k_2(a - b))\Big(\left(k_0{}^2 + k_1{}^2\right) \sin(ak_1) + 2ik_0 k_1 \cos(ak_1)\Big). \tag{4.10g}$$

As before, the scattering data consists of measurements of δu_- at $x = 0$ for wave numbers $k_0 \in [0, k_{\max}]$, where $k_{\max}a = 3$:

$$\delta u_-(0) = R_1. \tag{4.11}$$

We now present the results of numerical reconstructions. When computing the inverse Bremmer series, we use recursion to implement the formula (3.3). The scattering data is computed from (4.5). The forward operators are implemented using the formula (2.30). We compute the pseudo-inverse $\mathcal{K}_1 = K_{12}^+$, by using MATLAB's built-in singular value decomposition. Since the singular values of K_{12} are exponentially small, we set all but the largest M singular values to zero, and make use of only the first M. We discretize the integral operators on a spatial grid of N uniformly-spaced nodes. The choices of the parameters M, N are indicated in the figure captions. In each case, we found that increasing the number of spatial grid points did not significantly change the reconstructions.

In Figs. 1, 2 and 3 we show a series of reconstructions for scatterers of narrow support with variable levels of contrast in $\|\eta\|_{L^\infty(X)}$. In each case, the inverse series is computed to fifth order (five terms). Along with reconstructions of η, we also show the projection of η onto the subspace spanned by the first M singular vectors. The projection is, in some sense, the best approximation to η that can be obtained for a particular regularization. Note that for low contrast, the series appears to converge quite rapidly to a reconstruction that is close to the projection. At intermediate contrast, the higher order terms lead to significant improvements compared to the linear reconstructions. Evidently, the series diverges at high contrast.

In Figs. 4, 5 and 6 we repeat the numerical experiments described above, but for scatterers of wider support. The same qualitative picture holds, with the important caveat that there is
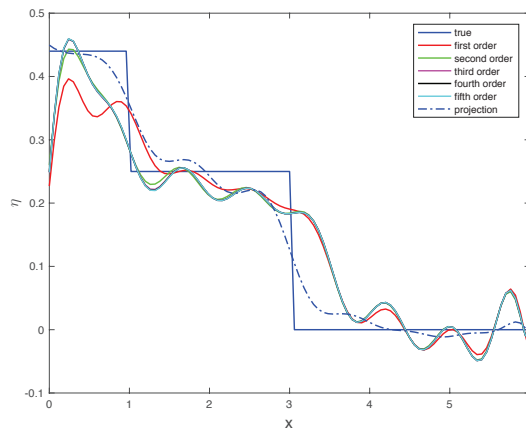
Fig. 4.1. Low contrast ($\|\eta\|_{L^\infty(X)} \simeq 0.6$), narrow support ($a = 1$), number of mesh points $N = 101$, $M = 15$ singular values were used for regularization, and $k_{\max}a = 3$.
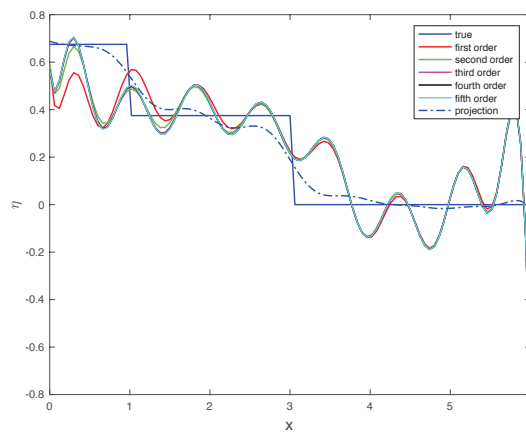
Fig. 4.2. Medium contrast ($\|\eta\|_{L^\infty(X)} \simeq 1.8$), narrow support ($a = 1$), number of mesh points $N = 101$, $M = 15$ singular values were used for regularization, and $k_{\max}a = 3$.

an interplay between the contrast and support. That is, for wider support, the series converges for lower contrast, consistent with Proposition 1 and the error estimate (40).

In Figs. 7, 8 and 9 we perform numerical experiments for the scatterer whose susceptibility is given by (4.6). By varying the contrast, we find that a similar picture as before obtains. Namely, the series converges for lower contrast and begins to diverge as the contrast increases.

5. Discussion

In conclusion, we have investigated the convergence of the inverse Bremmer series for scalar waves in one dimension. Exact solutions to the forward problem were used as scattering data and reconstructions were computed to fifth order in the inverse series. We found that the series converges quite rapidly for scatterers with relatively small contrast and support.

In future work, we plan to study the three-dimensional problem. In order to obtain an analogous hybrid-Bremmer series, it is necessary to select a preferred direction (the z-direction
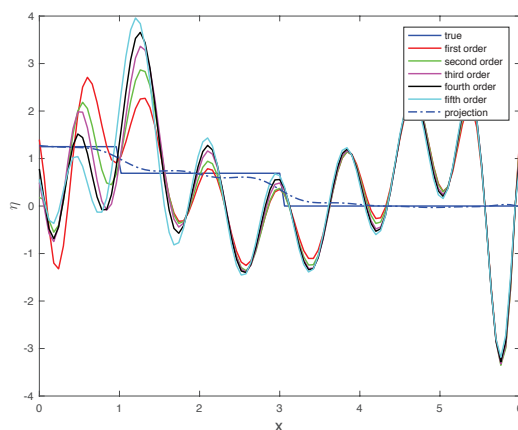
Fig. 4.3. High contrast ($\|\eta\|_{L^\infty(X)} \simeq 5.4$), narrow support ($a = 1$), number of mesh points $N = 101$, $M = 12$ singular values were used for regularization, and $k_{\max}a = 3$.
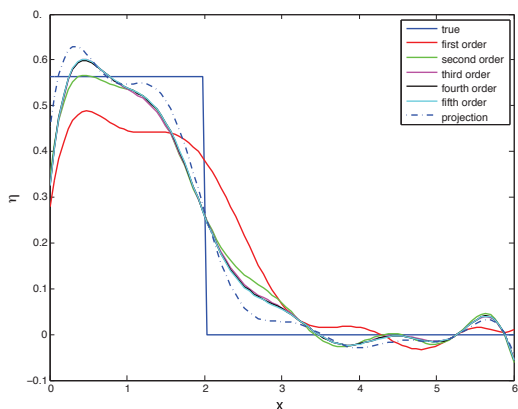
Fig. 4.4. Low contrast ($\|\eta\|_{L^\infty(X)} \simeq 0.6$), wide support ($a = 2$), number of mesh points $N = 101$, $M = 9$ singular values were used for regularization and $k_{\max}a = 3$.
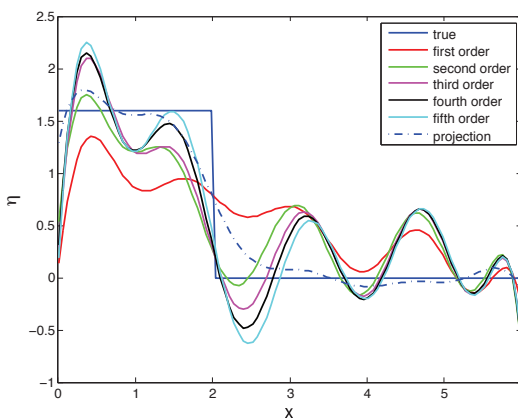
Fig. 4.5. Medium contrast ($\|\eta\|_{L^\infty(X)} \simeq 1.8$), wide support ($a = 2$), number of mesh points $N = 101$, $M = 9$ singular values were used for regularization, and $k_{\max}a = 3$.

for example). The wave equation then takes the form

$$\frac{1}{c(z,x)^2} u_{tt} = u_{zz} + \Delta u, \tag{5.1}$$
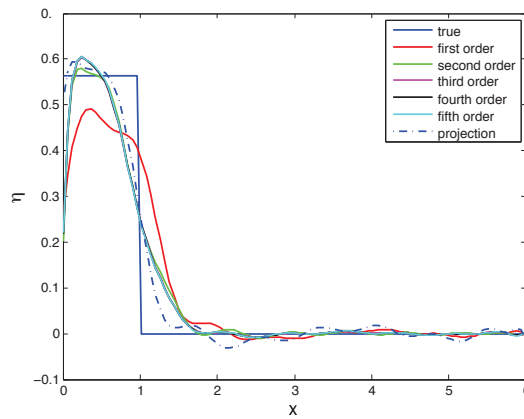
Fig. 4.6. High contrast ($\|\eta\|_{L^\infty(X)} \simeq 2$), wide support ($a = 2$), number of mesh points $N = 101$, $M = 9$ singular values were used for regularization, and $k_{\max}a = 3$.
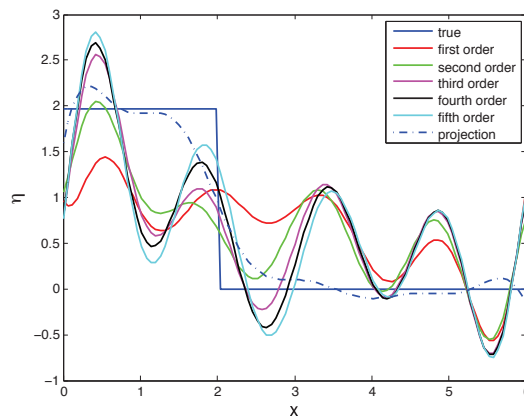
Fig. 4.7. η takes two low contrast values ($\eta \simeq 0.45$, for $0 \le x \le 1$ and $\eta \simeq 0.25$, for $1 < x \le 3$), number of mesh points $N = 101$, $M = 13$ singular values were used for regularization and $k_{\max}a = 3$.

where Δ is the Laplacian in the transverse direction. For simplicity, suppose that c depends only on the z coordinate, which corresponds to the case of a perfectly layered medium. Taking the Fourier transform of (5.1) in t and x we obtain

$$\hat{u}_{zz} + \left(\frac{\omega^2}{c(z)^2} - \xi^2 \right) \hat{u} = 0, \tag{5.2}$$

where ω is the Fourier variable conjugate to t, ξ is the Fourier variable conjugate to (x, y), and $\xi^2 = \xi_x^2 + \xi_y^2$. If we define

$$\eta(z, \xi) = \frac{c_0^2}{c(z)^2} - \frac{c_0^2 \xi^2}{\omega^2} - 1,$$

then (5.1) has the same form as (2.1). Thus, our results easily extend to the setting of a perfectly-layered medium. In the more general case where c depends on x and z, we can no longer take the Fourier transform of (5.1) in x in the usual sense, and $\eta(z, \xi)$ must be defined as a pseudo-differential operator. In this framework, the operator splitting is only approximate, which has implications for the construction of the Bremmer series [9].
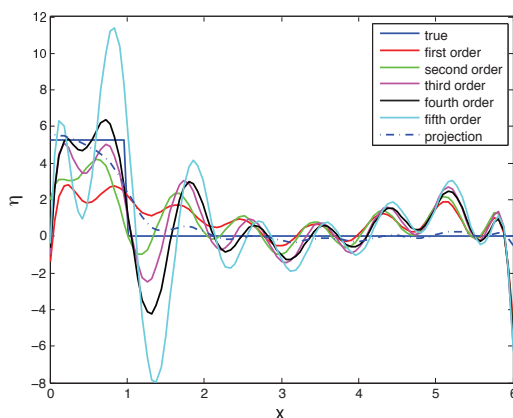
Fig. 5.1. η takes two medium contrast values ($\eta \simeq 0.7$, for $0 \leq x \leq 1$ and $\eta_{L^\infty(X)} \simeq 0.4$, for $1 < x \leq 3$), number of mesh points $N = 101$, $M = 11$ singular values were used for regularization, and $k_{\max}a = 3$.
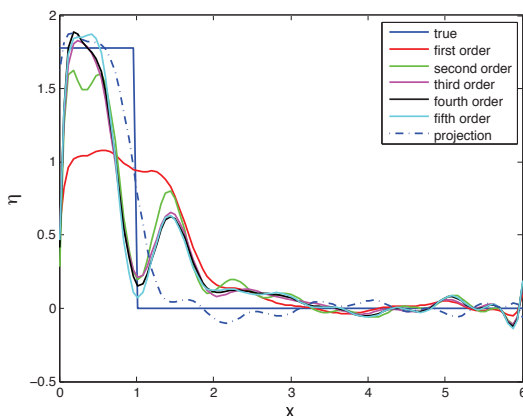
Fig. 5.2. η takes two high contrast values ($\eta \simeq 1.3$, for $0 \leq x \leq 1$ and $\eta \simeq 0.7$, for $1 < x \leq 3$), number of mesh points $N = 101$, $M = 10$ singular values were used for regularization, and $k_{\max}a = 3$. Reconstruction breaks down in this case.

References

[1] F. Cakoni and D. Colton, Qualitative Methods in Inverse Scattering Theory: An Introduction, Springer, 2005.

[2] K. Chadan and P. Sabatier, Inverse Problems in Quantum Scattering Theory, Springer, 1989.

[3] D. Colton and R. Kress, Inverse Acoustic and Electromagnetic Scattering Theory, Springer, 1992.

[4] S. Moskow and J.C. Schotland, Convergence and stability of the inverse scattering series for diffuse waves, *Inverse Problems*, **24** (2008), 065005 (16pp).

[5] S. Moskow and J.C. Schotland, Numerical studies of the inverse born series for diffuse waves, *Inverse Problems*, **25** (2009), 095007-25.

[6] M. Machida and J.C. Schotland, Inverse Born series for the radiative transport equation, *Inverse Problems*, **31**, (2015), 095009.

[7] K. Kilgore, S. Moskow and J.C. Schotland, Inverse Born series for scalar waves, *J. Comput. Math.*, **30**:6 (2012), 601-614.

[8] H. Bremmer, The WKB approximation as the first term of a geometric-optical series, *Commun. Pure Appl. Math.*, **4** (1951), 105-15.

[9] A.E. Malcolm and M.V. de Hoop, A method for inverse scattering based on the generalized Bremmer coupling series, *Inverse Problems*, **21** (2005), 1137-1167.

[10] T. Schuster, B. Kaltenbacher, B. Hofmann and K. Kazimierski, Regularization Methods in Banach Spaces (2012, De Gruyter, Berlin).

[11] T. Bonesky, K.S. Kazimierski, P. Maa, F. Schopfer and T. Schuster, Minimization of Tikhonov functionals in Banach spaces Abstr, *Appl. Anal.*, **2008** (2008), 1-20.